FATIGUE ASSESSMENT OF KNEE JOINTS SUBJECT TO TOTAL ARTHROPLASTY

Theodora Mouka[1], Dimitrios Vamvatsikos[2]

[1]School of Civil Engineering
National Technical University of Athens
Athens, GR-15780, Greece
e-mail: moukath@gmail.com

[2]School of Civil Engineering
National Technical University of Athens
Athens, GR-15780, Greece
e-mail: divamva@mail.ntua.gr, web page: http://users.ntua.gr/divamva

Keywords: Knee, Arthroplasty, Fatigue.

Abstract. *Total knee arthroplasty has become quite widespread, especially among patients of 70+ years. Unfortunately, failure of this surgery is not so uncommon. As a result, a revision surgery is sometimes needed, resulting in a great ordeal for patients. One of the major causes of this failure is the aseptic loosening of either the tibial or the femoral component, with that of the tibial component being more common. Our goal is to evaluate the performance of metallic knee implants used in total knee arthroplasty. More specifically, the aim is to identify critical areas of failure and the prevalent failure mechanisms due to fatigue. A probabilistic analysis will follow, in order to calculate the probability of failure as a function of walking cycles and loads on the knee joint.In the end, it will become possible to predict the likelihood of implant failure in the course of a patient's lifetime. It will also be possible to determine the probability of failure depending on the patient's habits and, as a result, how much the patient is allowed to stress the joint after the surgery depending on his/her weight. Similarly, the calculations will offer decision support on how much, if any, weight he/she should lose in order to lessen the probability of failure to an acceptable level. Ultimately, rehabilitation becomes more patient-specific and, therefore, likely much easier and less time-consuming.*

1 INTRODUCTION

Total knee arthroplasty has become quite widespread throughout the years. One of the reasons for this increasing popularity is the ever increasing life expectancy, leading to aging of the world population[1]. Unfortunately, failure of knee implants has occurred in quite a few cases. Result of such a failure is the need for a revision surgery, which leads to a great ordeal for patients.

One of the most common causes of failure is aseptic loosening of the tibial component [1], [2], [3], [4], [5]. Hazelwood et al[3] report early aseptic loosening of the tibial component due to cement-implant interface de-bonding, occurring at 0.36% of the Total Knee Replacements (TKRs) studied from May 2005 to December 2010. This percentage is remarkably low compared to other reports. Piedade et al[1] report a failure percentage of 2.33% due to aseptic loosening (between March 1988 and August 2002), while in earlier years (1974-1977) up to 26% of the knee replacement surgeries studied by Knutson et al[5] showed signs of loosening within 3 years after the operation. Although these reports indicate a certain improvement in the efficiency of knee arthroplasty over the years, it is clear that the problem still remains.

Part of the uncertainty that characterizes the problem lays in the scatter of the properties of bone cement, that is, the adhesive material that stabilizes the implant in the bone. The causes of failure have not yet been completely understood. Fatigue of the cement mantle is one of the main suspects[6],[7], there is controversy though on whether the failure initiates at the cement-bone interface, the cement-implant interface or within the cement mantle itself. Hazelwood et al[3] report early failure at the cement-implant interface, while van de Groes et al[8] find that the cement-bone interface is weaker and, therefore, more likely to fail.

Aim of this study is to identify the critical areas of failure and the prevalent failure mechanisms of the tibial component and assess its fatigue life.

2 MATERIALS AND METHODS

The first step in this study was to calculate the loads on a knee joint during a full gait cycle. An OpenSim[9] lower extremity model, developed by Lerner et al[10], was used for this purpose. The resulting load histories were subsequently used as excitation in an OpenSees[11] model of a tibial component, in order to calculate resulting stresses at the bone cement. These were then used in a fatigue analysis aiming to assess the fatigue life of the modeled implant. An ultimate limit state analysis was also performed. For this last part (ultimate limit state and fatigue analysis) a specifically developed MATLAB[12] code was employed.

2.1 OpenSim Model

OpenSim[9] is free software for musculoskeletal simulation. Using it, loads on the knee can be predicted with relative accuracy, taking into account not only the subject's weight, but also muscle forces and the position of the ligaments. The model developed by Lerner et al[10] (Fig. 1) was considered to be the most appropriate for the purposes of this study because it simulates the musculoskeletal system of the lower extremity and also allows subject-specific simulation of tibiofemoral alignment and geometry of the knee joint. The model was scaled and the appropriate analyses were run using the already existing data, which correspond to an adult male of 72.6kg, walking at a self-selected speed. In the end, a "JointReaction" analysis was run, in order to calculate loads on the knee joint during a gait cycle of the specific subject. Thus, load time histories of forces and joint moments were calculated in all three directions during a full gate cycle.

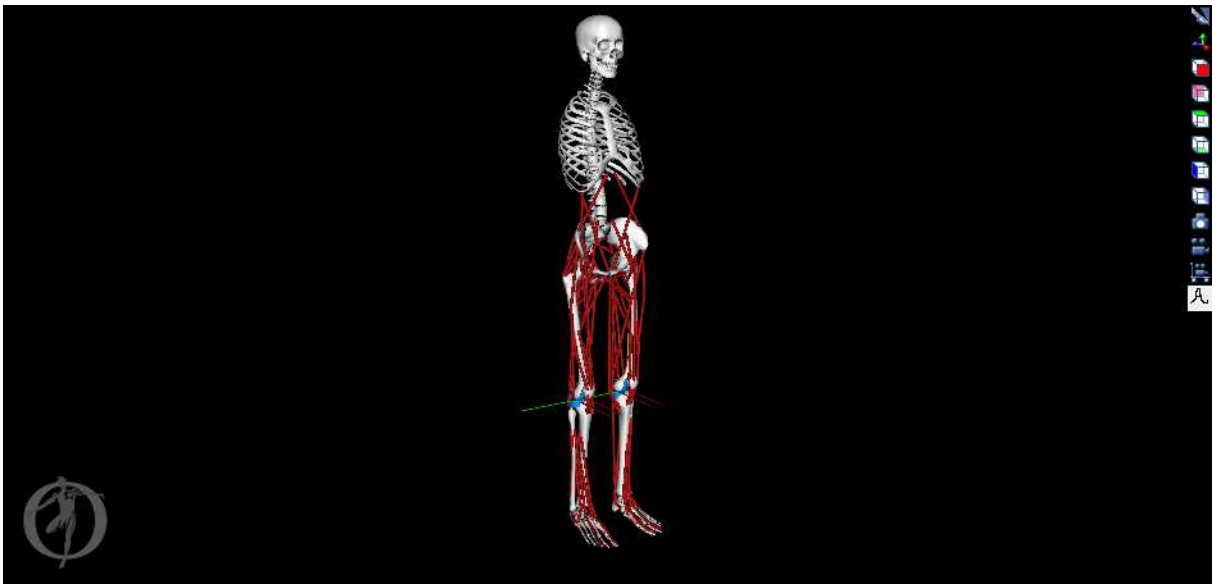

Figure 1. OpenSim[1] model by Lerner et al[6]

2.2 OpenSees Model

An effort was been made to use a simple model for reduced computational loads. Thus, a simplified 2-D model of a tibial component was created in OpenSees[11], using elastic materials. A typical geometry of a tibial component appears in Fig. 2, while the corresponding OpenSees model representing a medium-sized implant is shown in Fig. 3. The Young's modulus of the tibial component was assumed to be equal to 210000MPa and that of the bone cement 2200MPa[13]. The cement-implant interface, the cement mantle and the cement-bone interface were simulated with elastic uniaxial springs placed in series to generate compound spring elements. Two independent compound springs were placed every 2mm along the implant-bone boundary, in order to account for both normal and shear stresses at the interfaces. Interface stiffness values were taken from literature[13] and can be seen in Table 1. Spring stiffness was calculated by multiplying every interface stiffness value with the area corresponding to each spring. Said area is different for the tibial plate (horizontal part) and stem (vertical part) of the implant, due to the difference in geometry of the two parts. Resulting stiffness values can be seen in Table 2.

The model was subsequently subjected to the load time histories that were estimated from the OpenSim "JointReaction" analysis. This analysis calculates loads in all three directions, though only those acting on the plane of the model (coronal plane) were inserted in the OpenSees analysis (Fig. 3). After the analysis in OpenSees was run, the individual spring force time histories were obtained. Since each spring represents a fraction of a surface, the area of which is predetermined, these forces were easily converted to corresponding stresses, which were then used in the fatigue and ultimate state analyses.

Figure 2. Typical geometry of a tibial compartment (AMPLITUDE ANATOMIC®)

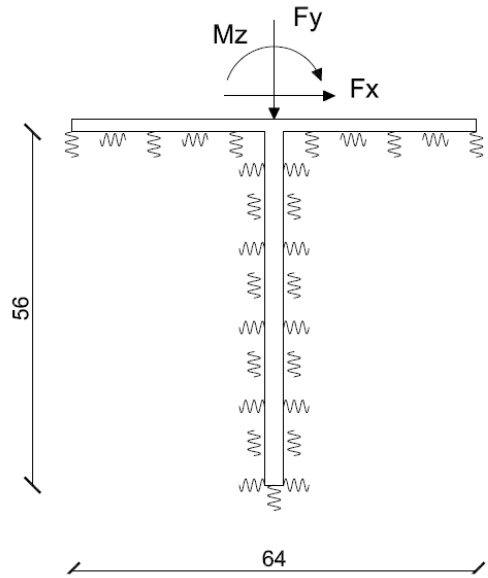

Figure 3. Schematic picture of the tibial implant model (dimensions in mm)

	Stiffness in tension MPa/mm	Stiffness in compression MPa/mm	Shear Stiffness MPa/mm
Implant-cement interface	57.3	5730.0	151.4
Cement-bone interface	37.4	3740.0	38.4

Table 1 : Interface stiffness values

	Stiffness in tension kN/mm	Stiffness in compression kN/mm	Shear Stiffness kN/mm
	Plate		
Implant-cement interface	6.42	641.76	16.96
Cement-bone interface	4.19	418.88	4.30
	Stem		
Implant-cement interface	2.70	270.02	3.23
Cement-bone interface	1.76	176.24	1.81

Table 2 : Spring stiffness values

2.3 Ultimate State and Fatigue Analysis

The ultimate state and fatigue analyses were performed by means of a specifically developed MATLAB code. The first part of the code was to convert the resulting OpenSees spring forces into their corresponding stresses. Thus, both a normal and a shear stress history was obtained for each area fraction simulated with a spring element. These stresses were then used for the subsequent analyses.

As far as the ultimate state analysis is concerned, only the cement-bone interface was initially examined as it is considered to be weaker than both the cement-implant interface and the cement mantle[8]. Normal and shear strength values were obtained from the literature[13],[8]. Specifically, the strength values provided for cement-cancellous bone interface were used (tensile S_t=1.79 ± 0.82 MPa, shear S_s=3.85 ± 1.87 MPa, compressive S_c=70MPa). Tensile and shear strengths are the most critical and can vary considerably. Therefore, it was considered more realistic to assume a random tensile and shear strength for each surface fraction, with the aforementioned corresponding mean and standard deviation. Both variables (S_t and S_s) were assumed to be normally distributed, while a lower and upper limit were also incorporated to truncate the tails so that negative or

excessively high values are removed. These limits were estimated taking into account experimental data by Mann et al[14], [15] and can be seen in Table 3.

	S_t (MPa)	S_s (MPa)
Lower limit	0.25	0.5
Upper limit	3.0	5.0

Table 3 : Strength Limits

Subsequently, an ultimate state analysis was performed separately for each element, employing the Tsai-Hill failure criterion, which is simplified significantly in this case (Eqs. (1) and (2)) [15]:

$$\sigma \geq 0 \rightarrow \quad \frac{\sigma^2}{S_t^2} + \frac{\tau^2}{S_s^2} \leq 1 \tag{1}$$

$$\sigma \leq 0 \rightarrow \quad \frac{\sigma^2}{S_c^2} + \frac{\tau^2}{S_s^2} \leq 1, \tag{2}$$

where σ stands for normal and τ for shear stress. The selection of this particular criterion was due to its more realistic results in comparison with other criteria proposed in literature. A linear or a Hoffmann failure criterion, which are used in other studies[8], [16], tended to produce too conservative results in this study (even immediate failure) and therefore were judged to be unrealistic.

As far as the fatigue analysis is concerned, only the normal stress time history for each element was taken into account, because there is insufficient data on multiaxial fatigue properties of bone cement. Cycles (N) and amplitudes ($\Delta\sigma$) were counted by means of the rainflow algorithm, employing an already existing MATLAB code developed by A. Niesłony[17]. Finding an appropriate and realistic S-N curve in order to proceed with the calculation of cycles to failure (N_f) was quite taxing because of the scatter in fatigue data. Few studies have been produced on fatigue of the various bone cement types (Jeffers et al[6], Murphy and Prendergast[18], Sheafi[19], Tanner et al[20]) and fewer still on fatigue of the implant-cement and cement-bone interfaces (Kim et al[21]). A normalization of some of the proposed curves was attempted in order to take into account the actual strength of the interfaces, but with no realistic results. This is attributed to the tremendous scatter of experimental fatigue data and also to the fact that most of these curves were developed by testing bone cement specimens, not interfaces. As a result, again the curve producing the most realistic results was employed. Said curve (Eq. (3)) was proposed by Murphy and Prendergast[18] for vacuum-mixed cement.

$$\Delta\sigma = -2.86\log\left(N_f\right) + 33.06 \tag{3}$$

After calculating the cycles to failure (N_f) for each given stress amplitude ($\Delta\sigma$), the damage accumulation (D) was calculated using the Palmgren-Miner rule:

$$D = \sum_{i=1}^{n} \frac{N_i}{N_f\left(\Delta\sigma_i\right)}, \tag{4}$$

where n stands for the number of different amplitudes resulting from rainflow counting. Number of cycles N_i for each stress level occurred under the assumption that the patient walks for half an hour per day on average. When $D = 1$, it is assumed that the corresponding element has failed and, subsequently, its fatigue life is exhausted. When an element failed, the OpenSees analysis was run again, with that particular element having 1% of its original stiffness. The same procedure was repeated until all elements had failed. In the end, the total fatigue life of the implant was calculated.

3 RESULTS

Forces acting on the right tibia during a gait cycle were obtained from the OpenSim “JointReaction” analysis and can be seen in Figures 4 to 6. Only forces acting on the plane of the OpenSees model are shown. It is clear that the resulting force on the joint can easily reach a value equal to three times the patient’s body weight. This leads to high values of compressive stress at the cement mantle. Peak observed value of compressive stress was σ_c = 20.6MPa around the middle of the tibial plate (Fig. 7), peak tensile stress σ_t = 0.65MPa at the lateral side of the tibial plate (Fig. 8) and peak shear stress τ = 0.46MPa at the proximal end of the stem (Fig. 9). These values correspond to the time before the beginning of any local fatigue failure, while the cement mantle is still intact.

Results of the failure analysis can be seen in Fig. 10. Assuming a moderate walking activity pattern for the patient, failure of the first element occurs in 7.25 years after surgery and recovery, while total failure of the implant occurs in 9.1 years. The most critical area (that is, the area of failure initiation) appears to be located near the middle of the tibial plate. Fatigue seems to be the main cause of this failure. The area where peak tensile stress occurs is also critical, since it tends to fail immediately if its tensile strength is below average.

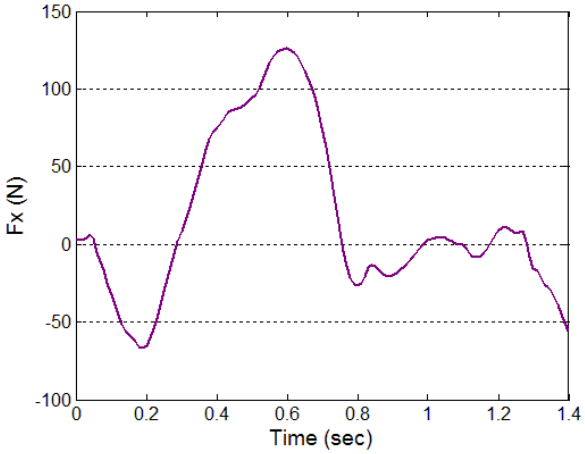

Figure 4. F_x during a gait cycle

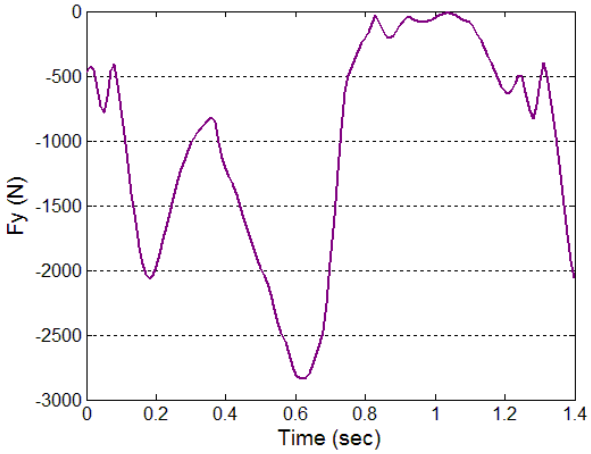

Figure 5. F_y during a gait cycle

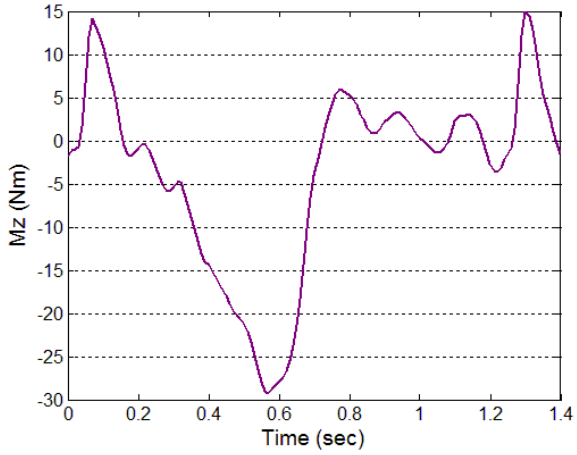

Figure 6. M_z during a gait cycle

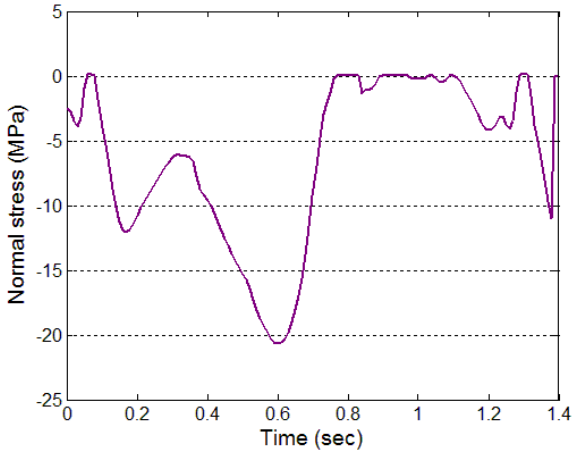

Figure 7. Stress history at the area of peak compressive stress occurrence

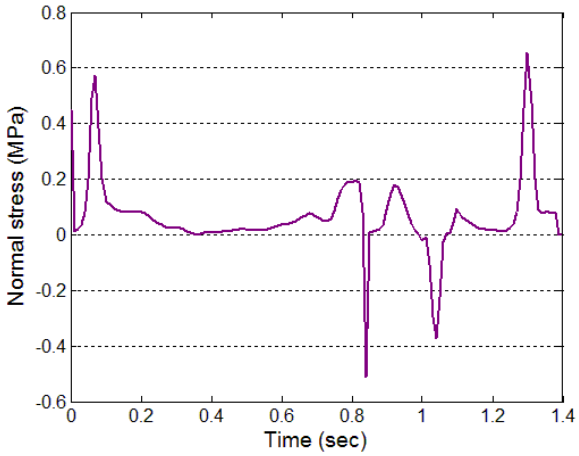

Figure 8. Stress history at the area of peak tensile stress occurrence

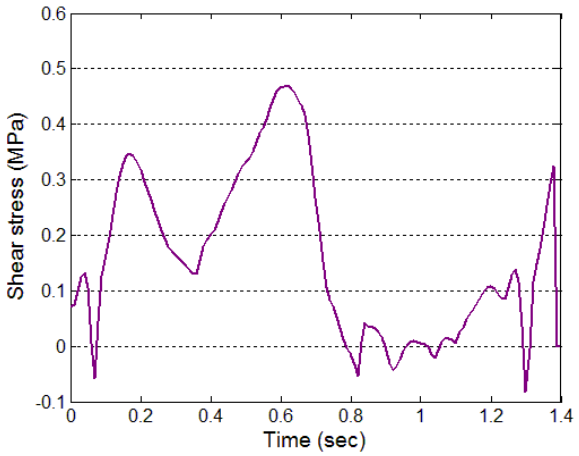

Figure 9. Stress history at the area of peak shear stress occurrence

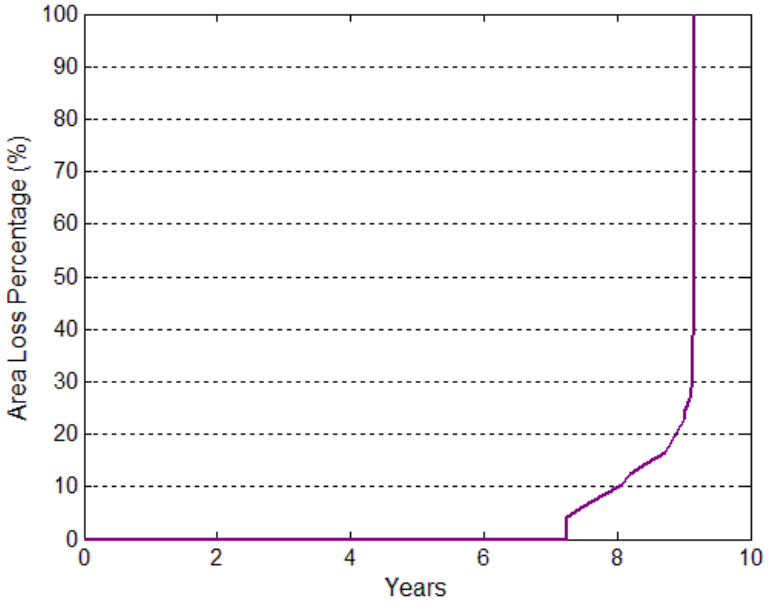

Figure 10. Cement area loss at the implant-bone boundary as a function of time

4 DISCUSSION

Each spring element used in this study incorporates the cement-implant interface, cement mantle and cement-bone interface. Which of those fails first is a challenge to predict and depends greatly on cement properties at each point. Interfaces are generally more susceptible to failure and, according to current literature[8],[21], bone-cement interface seems to be weaker than cement-implant interface. Therefore it should be the first that fails, but in vivo de-bonding seems to happen mostly at the cement-implant interface. An explanation of this paradox may be provided by the fact that, since the bone consists of living tissue, it may be capable of mending the microcracks occurring at the bone-cement interface under loads of everyday life[21]. This implies that cement-bone interface may not be the most critical to failure. On the other hand, the critical area of failure initiation is clearly located near the middle of the tibial plate, which is where the highest compressive stress values occur. Due to the sensitivity of bone cement and interfaces in tensile stresses, the lateral side of the tibial plate is also susceptible to failure if the tensile strength at that point is relatively low, since the tensile stress values occurring at this area are relatively high.

As far as fatigue life is concerned, early failure of tibial implants is unlikely to happen if there is no pre-existing flaw in the cement mantle. Still, their life span depends on many parameters, such as innate flaws in the cement mantle or differentiation of its strength. The patient's lifestyle is also important, since it affects the expected loads on the knee joint. Moreover, uncertainty of fatigue properties of bone cement is also an issue, more so because, apart from the scatter that characterizes fatigue data of all materials, they also depend on the mixing method, viscosity, penetration, amount of interdigitation in the bone-cement interface etc. Yet it is clear that the loads acting on the knee joint during the patient's everyday life result to high stress values at the cement, often reaching an important fraction of its strength. This is consistent with other studies (van de Groes et al[8]) and can lead to reduced fatigue life. Moreover, it seems that it takes almost 2 years from the initiation of failure until the implant becomes completely loose. Nevertheless, it is likely that, at some point, enough de-bonding has occurred to allow mediolateral movement of the implant, which would exacerbate and accelerate loosening.

In conclusion, results of this study can be used for an initial estimation of the expected life span of such an implant, though there is definitely potential of improvement in accuracy if more accurate implant geometry and cement fatigue and strength data are provided. Yet the possibilities are infinite, since this methodology can provide patient-specific treatment and rehabilitation data, fully adapting to the gait, weight and lifestyle of the subject.

REFERENCES

[1] Piedade, S.R., Pinaroli, A., Servien, E., Neyret, P. (2008), "Revision after early aseptic failures in primary total knee arthroplasty," Knee Surgery Sports Traumatology Arthroscopy, 17, pp. 248-253.

[2] Foran, J.R.H., Whited, B.W., Sporer, S.M. (2011), "Early aseptic loosening with a precoated low-profile tibial component-A case series," The Journal of Arthroplasty, 26(8), pp. 1445-1450.

[3] Hazelwood, K., O'Rourke, M., Stamos, V., McMillan, R., Beigler, D., Robb W. III (2015). "Case series report: Early cement–implant interface fixation failure in total knee replacement," The Knee, 22(5), pp. 424-428.

[4] Hoey, D., Taylor, D. (2009), "Statistical distribution of the fatigue strength of porous bone cement," Biomaterials, 30, 6309-6317.

[5] Knutson, K., Jónsson, G., Langer Andersen, J., Lárusdóttir, H., Lidgren, L. (1981). "Deformation and loosening of the tibial component in knee arthroplasty with unicompartmental endoprostheses." Acta Orthopaedica Scandinavica, 52(6), 667-673.

[6] Jeffers, J.R.T., Browne, M., Taylor, M. (2005), "Damage accumulation, fatigue and creep behavior of vacuum mixed bone cement," Biomaterials, 26, pp. 5532-5541.

[7] Topoleski, L.D.T., Ducheyne, P., Cukler, J.M. (1990), "A fractographic analysis of in vivo poly(methyl methacrylate) bone cement failure mechanisms," Journal of Biomedical Materials Research, 24(2), pp. 135-154.

[8] van de Groes, S., de Waal Malefijt, M., Verdonschot, N. (2014), "Probability of mechanical loosening of the femoral component in high flexion total knee arthroplasty can be reduced by rather simple surgical techniques," The Knee, 21, pp. 209-215.

[9] Delp, S.L., Anderson, F.C., Arnold, A.S., Loan, P., Habib, A., John, C.T., Guendelman, E., Thelen, D.G. (2007) , "OpenSim: Open-source software to create and analyze dynamic simulations of movement," IEEE Transactions on Biomedical Engineering, 54(11), pp. 1940-1950. [URL http://opensim.stanford.edu/]

[10] Lerner, Z., DeMers, M., Delp, S., Browning, R. (2015), "How tibiofemoral alignment and contact locations affect predictions of medial and lateral tibiofemoral contact forces," Journal of Biomechanics, 48(4), pp. 644-650.

[11] McKenna, F., Fenves, G.L., Scott, M.H. (2000), "Open system for earthquake engineering simulation," University of California, Berkeley, CA. [URL http://opensees.berkeley.edu/]

[12] MATLAB version 7.12.0, The Mathworks Inc. (2011), Natick, Massachusetts, United States

[13] van de Groes, S.A.W., de Waal Malefijt, M., Verdonschot, N. (2013), "Influence of preparation techniques to the strength of the bone-cement interface behind the flange in total knee arthroplasty," The Knee, 20, pp. 186-190.

[14] Mann, K.A., Ayers, D.C., Werner, F.W., Nicoletta, R.J., Fortino, M.D. (1997), "Tensile strength of the cement-bone interface depends on the amount of bone interdigitated with PMMA cement," Journal of Biomechanics, 30(4), pp. 339-346.

[15] Mann, K.A., Mocarski, R., Damron, L.A., Allen, M.J., Ayers, D.C. (2001), "Mixed-mode failure response of the cement-bone interface," Journal of Orthopaedic Research, 19, pp. 1153-1161.

[16] Zelle, J., Janssen, D., Peeters, S., Brouwer, C., Verdonschot, N. (2011), "Mixed-mode failure strength of implant-cement interface specimens with varying surface roughness," Journal of Biomechanics, 44, pp. 780-783.

[17] Niesłony, A. (2009), "Determination of fragments of multiaxial service loading strongly influencing the fatigue of machine components," Mechanical Systems and Signal Processing, 23(8), pp. 2712-2721.

[18] Murphy, B.P., Prendergast, P.J. (2000), "On the magnitude and variability of fatigue strength of acrylic bone cement," International Journal of Fatigue, 22, pp. 855-864.

[19] Sheafi, E.A.M. (2015), "Effects of various test regimes on fatigue behaviour of PMMA bone cement: a comparative study," PhD Thesis, University of Glascow.

[20] Tanner, K.E., Wang, J.-S., Kjellson, F., Lidgren, L. (2010), "Comparison of two methods of fatigue testing bone cement," Acta Biomaterialia, 6, pp. 943-952.

[21] Kim, D.-G., Miller, M.A., Mann, K.A. (2004), "Creep dominates tensile fatigue damage of the cement-bone interface," Journal of Orthopaedic Research, 22, pp. 633-640.